

# Deep Learning Predictors for Traffic Flows

Nicholas G. Polson  
*Booth School of Business*  
*University of Chicago\**

Vadim O. Sokolov  
*Center for Transportation Research*  
*Argonne National Laboratory*

First Draft: December 2015  
This Draft: April 2016

## Abstract

We develop a deep learning predictor for modeling traffic flows. The challenge arises as traffic flows have sharp nonlinearities resulting from transitions from free flow to breakdown and then to congested flow. Our methodology uses a deep learning architecture to capture nonlinear spatio-temporal flow effects. We show how traffic flow data, from road sensors, can be predicted using deep learning. For comparison, we use a benchmark sparse  $\ell_1$  trend filter and we illustrate our methodology on traffic data from Chicago's Interstate I-55. We focus on forecasting traffic flows during special events, such as a Chicago Bears football game and an extreme snowstorm, where the sharp traffic flow regime can occur very suddenly and hardly predictable from historical patterns. Finally, we discuss directions for future research.

## 1 Introduction

### 1.1 Traffic Flow Prediction

Traffic flow forecasting uses real-time measurements of traffic flow speed that are available from in-ground loop detectors or GPS probes. The main difference is that the spatial distribution of measurements depends on the sensing methodology. Bing Maps relies on both sources of data, and then uses probabilistic graphical modeling to predict speeds for each road segment [Microsoft Research (2016)]. The goal of our paper is to develop near real-time forecasting for a window

---

\*Polson is Professor of Econometrics and Statistics at the Chicago Booth School of Business. email: [ngp@chicagobooth.edu](mailto:ngp@chicagobooth.edu). Sokolov is a principal computational scientist at Argonne National Laboratory, email: [vsokolov@anl.gov](mailto:vsokolov@anl.gov)

of at most forty minutes. The forecasting model depends on the number of road segments in the network, frequency of measurements and number of sensors. The challenges in traffic forecasts, for large scale networks, are identifying the dependency structure between the model variables to representing sharp discontinuities in data. For example, there are 20,000 highway and major arterial road segments in the Chicago metropolitan area. Thus, it is required to develop a forecast using tens of thousands of predictors in nearly real time. Previous methods are typically applicable to small size networks and model selection mechanism is done in an ad-hoc manner.

To solve the predictor selection problem we use hierarchical sparse vector auto regressive techniques [Dellaportas et al. (2012); Nicholson et al. (2014)]. To model the discontinuities in traffic flow we use a deep learning model which forecasts traffic flow as a superposition of univariate non-linear actuator functions with affine arguments. Both models are scalable and can be estimated using a traditional optimization technique such as stochastic gradient descent. Predictor selection in our deep learning formulation is performed using dropout Hinton and Salakhutdinov (2006).

The goal of our paper is to capture nonlinear spatio-temporal effects in both recurrent and non-recurrent traffic congestions that arise due to conditions such as work zones, weather, special events, and traffic incidents. All of these factors introduce travel time uncertainty and need to be forecast. Traffic managers use model-based forecasts to regulate ramp metering, apply speed harmonization, and change road pricing as congestion mitigation strategies; whereas, the general public adjusts its decisions on departure times and travel route choices, among other things. Nonlinearities present in traffic flows [Kamarianakis et al. (2010)] need to be properly modeled. Layered hierarchical models such as neural networks are commonly used to develop short term traffic forecasts. Karlaftis and Vlahogianni (2011) provide an overview of previously developed approaches. The simplest version of a neural network, a network with no hidden layers, is equivalent to linear regression. It was noted previously by Kamarianakis et al. (2012) that model training is computationally expensive, and frequent model updating is prohibitive. As we show later in Section 3.1 our estimation procedure leads to an efficient methodology for finding a sparse model that can be frequently updated in nearly real time.

We present a deep learning predictor for spatial-temporal relations present in traffic speed measurements. Our model can be used to forecast congestion propagation, given a bottleneck location, and we provide forty minute speed forecasts for days with recurrent and non-recurrent traffic conditions. Our deep learning predictor can incorporate data sources, such as weather forecasts and police reports to produce more accurate forecasts. We illustrate our methodology on traffic flows during special events. For example, we analyze traffic patterns around a Chicago bears football game and an extreme snow storm. For previous studies, see Anacleto et al. (2013); Blandin et al. (2012); Chiou et al. (2014); Polson and Sokolov (2015, 2014); Work et al. (2010).

The rest of the paper is outlined as follows. Section 1.2 provides connection with existing work. Section 1.3 reviews fundamental basics of deep learning. Section 2 develops our deep learning predictors for forecasting traffic flows. Section 3 discusses fundamental characteristics of traffic flow data and illustrates our methodology with study of traffic flow on Chicago's I-55. Finally, Section 4 concludes with directions for future research.

## 1.2 Connections with Existing Work

Short-term traffic flow predictions has a well studied history in the transportation literature. Our approach builds on the regularized Bayesian methodology, for transportation applications see Tebaldi and West (1998) who infer network route flows. Westgate et al. (2013) study travel time reliability for ambulances using noisy GPS for both path travel time and individual road segment travel time distributions. Anacleto et al. (2013) develop a dynamic Bayesian network to model external intervention techniques to accommodate situations with suddenly changing traffic variables.

Neural networks, have been widely applied and shown to be particularly successful in traffic pattern recognition, see, for example Ripley (1996); Lv et al. (2015). Shallow neural network-based approach for traffic applications was proposed in Chen and Grant-Muller (2001), the authors propose a memory efficient dynamic neural network based on resource allocating network (RAN). The model had a single hidden layer with Gaussian radial basis function activation units. Zheng et al. (2006) proposes several one-hidden layer networks to produce fifteen minute forecasts. Two types of networks were considered, one with tanh activation function and another with Gaussian radial basis function. Then several forecasts were combined using a Bayes factor that calculates an odds ratio for each of the models dynamically. A state-space neural network was proposed in Van Lint et al. (2005). An approach that uses day of the week and time of day as inputs for a neural network was proposed in Çetiner et al. (2010). We add to this line of research by showing an additional advantage of deep hidden layers together with sparse autoregressive techniques. Breiman (2003) agrees that neural networks provide more flexibility than traditional statistical methods.

## 1.3 Deep Learning

The fundamental deep learning problem is to find a predictor of an output  $y$  given an input  $x$ . The class of deep learning predictors  $\hat{y}(x)$  are constructed by composition. Let  $f$  be a given *univariate* activation function. A semi-affine activation rule is then defined by

$$f_{w_l, b_l}(x) = f\left(\sum_{j=1}^{N_l} w_{lj} x_j + b_l\right) = f(w_l^T x_l + b_l) \quad (l = 1, \dots, n). \quad (1)$$

Our deep predictor, is the composite map

$$F(x) = \hat{y}(x) = (f_{w_n, b_n} \circ \dots \circ f_{w_1, b_1})(x).$$

that approximates original unknown function  $F(x)$ . Poincare and Hilbert showed that there exists an activation function that is a universal basis. The main advantage of using deep hidden layers is that  $x$  can be high dimensional but the activation functions are univariate. This implicitly needs the specification of the number of hidden units  $N_l$  for each layer  $l$ . We still need to solve the training problem of finding  $(\hat{w}, \hat{b})$  and implicitly  $N_l, n$  – the model selection problem.

Modern deep learning techniques are rooted in Kolmogorov–Arnold’s representation theorem [Kolmogorov (1956)]. The theorem states that any continuous function of  $n$  variables  $F(x)$ , where  $x = (x_1, \dots, x_n)$ , can be represented as  $F(x) = \sum_{j=1}^{2n+1} g_j(\sum_{i=1}^n h_{ij}(x_i))$ , where  $g_j$  and  $h_{ij}$  are continuous functions, and  $h_{ij}$  is a universal basis, that does not depend on  $F$ . This remarkable representation implies that any continuous function can be represented using operations of summation and function composition. For a neural network, it means that any function of  $n$  variables

can be represented as a neural network with one hidden layer and  $2n + 1$  activation units. The difference between theorem and neural network representations is that functions  $h_{ij}$  are not necessarily affine. Further, it is not clear how to find such a basis. In their original work Kolmogorov and Arnold developed functions in a constructive fashion. It makes this theorem unusable for practical applications. Diaconis and Shahshahani (1984) characterize projection pursuit functions for a specific types of input functions  $F(x)$ .

Deep learning allows for efficient modeling of nonlinear functional representations. For example, principal components analysis Wold (1956); Cook (2007) for dimensionality reduction can be extended to a case when components are nonlinear functions of the data. Most of the recent improvements in large scale data analysis techniques come from applying scalable modern optimization and parallelization techniques, see Dean et al. (2012); Polson et al. (2015); Sra et al. (2012). Regularized Bayesian model fitting allows to develop a parsimonious scalable model, that make frequent updating feasible. Our methodology, provides an alternative to previously proposed time-series methods and traditional state-space models for forecasting.

## 2 Deep Learning for Traffic Flow Prediction

We now turn to the problem of developing a deep learning predictor for traffic flow analysis. For traffic flow model previously measured and possibly filtered traffic flow data given by  $x^t = (x_{t-k}, \dots, x_t)$  used as regressors. The goal in traffic flow forecasting is to build a model  $x_{t+h}^t = \hat{y}(x^t)$ , here  $\hat{y}$  is a parametrized superposition of univariate non-linear functions with affine arguments and  $x_{t+h}^t$  is the forecast traffic flow speeds at time  $t + h$ , given measurements up to time  $t$ .

Thus, we consider a non-linear deep learning model for  $\hat{y}$ . Consider a neural network with  $n$  hidden layers. Let  $l = 1, \dots, n$  be then index for the layers. Let  $z^l$  denote the vector of inputs into a layer  $l$  and  $y^l$  denote the vector of outputs, then a feed-forward neural network model can be described as

$$\begin{aligned} z_i^{l+1} &= \sum_{i=1}^{N_l} (w_i^{l+1} y_i^l + b_i^{l+1}) \quad (i = 1, \dots, N_{l+1}) \\ y_i^{l+1} &= f(z_i^{l+1}) \quad (i = 1, \dots, N_{l+1}), \end{aligned}$$

here  $N_l$  is the number of activation units (neurons) at layer  $l$  and function  $f$  is called an activation function. Typical choices for an activation function include tanh and rectifier function  $f(x) = \max(0, x)$ . The forecast is  $x_{t+h}^t = y^n = (f(z_1^n), \dots, f(z_{N_n}^n))$ .

Suppose we wish to predict traffic flows 40 minutes in advance. The vector of interest is

$$x_{t+40}^t = \begin{pmatrix} x_{1,t+40} \\ \vdots \\ x_{L,t+40} \end{pmatrix},$$

where  $L$  is the number of locations on the network (loop detectors) and  $x_{i,t}$  is the traffic flow speed at location  $i$  at time  $t$ .

To develop the forecast we use input vector  $x^t \in \mathbb{R}^{TL}$ , where  $T$  is the number of lagged measurements to be used and  $L$  is the number of locations on the network at which measurements available. Thus,  $x^t$  contains recent measurements from each location on the network

$$x^t = \text{vec} \begin{pmatrix} x_{1,t-40} & \dots & x_{L,t} \\ \vdots & \vdots & \vdots \\ x_{L,t} & \dots & x_{L,t} \end{pmatrix}.$$

Here,  $\text{vec}$  is the vectorization transformation, which converts the matrix into a column vector. In our application examined later in Section 3.1, we have twenty one road segments (i.e.  $L = 21$ ) that span thirteen miles of a major corridor connecting Chicago’s southwest suburbs to the central business district. The chosen length is consistent with several current transportation corridor management deployments [TransNet (2016)].

We use a hierarchical linear vector autoregressive model to identify the spatio-temporal relations in the data. We consider the problem of finding sparse matrix  $A$  in the following model

$$x_{t+40}^t = Ax^t + v_t, \quad v_t \sim N(0, V);$$

here  $A$  is a matrix of size  $L \times Lk$ , and  $k$  is the number of previous measurements used to develop a forecast. In our example considered in Section 3.1 we have  $L = 21$ , however in large scale networks there are tens of thousands locations with measurements available.

Then problem of finding the spatio-temporal relations in the data is the predictor selection for linear models, such as vector autoregressive models. It is a well developed topic. Estimation algorithms for finding sparse models rely on adding a penalty term to a loss function. A recent review by Nicholson et al. (2014) considers several prominent scalar regularization terms to identify sparse vector auto-regressive models.

The predictors selected as a result of finding the liner model are then used to build a deep learning model. To find an optimal network (structure and weights) we used stochastic gradient descent (SGD) method implemented in the package `H2O`. Similar methods are available in `Python`’s `Theano` framework by Bastien et al. (2012). We generated  $10^5$  Monte Carlo samples from the following space:

$$\begin{aligned} f &\in \{\tanh(x), \max(x, 0)\} \\ n &\in \{1, \dots, 60\} \\ N_l &\in \{1, \dots, 200\}^n \\ \lambda &\in [10^{-4}, 10^{-2}] \\ x_{t+h}^t &= (f_n \circ \dots \circ f_1)(x^t), \quad f_l = f(w_l^T x_l + b_l). \end{aligned}$$

We used out-of-sample model performance as a criteria for selecting our final deep learning architecture.

## 2.1 Training

At a fundamental level, we use a training set  $(y_i, x_i)_{i=1}^N$  of input-output pairs, to train our deep learning model by minimizing the difference between training target  $y_i$  and our predictor  $\hat{y}(x_i)$ .

To do this we need a loss function,  $l(y, \hat{y})$  at the level of the output signal. When we have a traditional probabilistic model  $p(y \mid \hat{y})$  that generates the output  $y$  given the predictor  $\hat{y}$ , then we have the natural loss function  $l(y, \hat{y}) = -\log p(y \mid \hat{y})$ . For deep learning problems a typical  $\ell_2$  norm squared used as a loss function. It is common to add a regularization penalty  $\phi(w, b)$  that will avoid over-fitting and stabilize our predictive rule. To summarize, given an activation function, the statistical problem is to optimally find the weights and biases  $w = (w_0, \dots, w_n)$ ,  $b = (b_0, \dots, b_n)$  that minimize the loss function with  $\ell_2$  separable regularization term given by

$$\begin{aligned} (\hat{w}, \hat{b}) &\in \underset{w, b}{\operatorname{argmin}} \quad \|y - \hat{y}_{w, b}(x)\|_2^2 + \lambda \phi(w, b) \\ \phi(w, b) &= \|w\|^2 + \|b\|^2 \\ \hat{y}_{w, b}(x) &= (f_n \circ \dots \circ f_1)(x^t), \quad f_l(x) = f\left(\sum_{j=1}^{200} w_{lj}x_j + b_l\right), \end{aligned}$$

here  $w_l \in \mathbb{R}^{l-1}$ ,  $b_l \in \mathbb{R}$ , and  $\lambda$  gages the overall level of regularization. Choices of penalties for  $\phi(w, b)$  include the ridge penalty  $\ell_2$  or the lasso  $\ell_1$  penalty to induce sparsity in the weights. A typical method to solve the optimization problem is gradient descent. However, the caveats of this approach include poor treatment of multi-modality and slow convergence.

Models constructed from deep learning predictors can be fit easily to training data using a stochastic gradient descent (SGD) algorithm. However, from our experiments with the traffic data, we found that using sparse linear model estimation to identify spatial-temporal relations between variables, yield better results, as compared to using drop-out or regularization terms for neural network loss function.

In order to find optimal structure of the neural network (number of hidden layers  $n$ , number of activation units in each layer  $N_l$  and activation functions  $f$ ) as well as hyper-parameters, such as  $\ell_1$  regularization weight, we used a random search. Though this technique is inefficient for large scale problems, for the sake of exploring potential structures of the networks that deliver good results and can be scaled, this is an appropriate technique for small dimensions. An alternative to random search, that relies on genetic optimization algorithm for learning the network structure for traffic forecasts proposed in Vlahogianni et al. (2005).

## 2.2 Trend Filtering

The goal is to filter noisy data from physical sensors and then to develop model-based predictors. Iterative exponential smoothing is a popular technique which is computationally efficient. It smoothers oscillations which occur on arterial roads with traffic signal controls, when measured speed is “flipping” between two values, depending whether the probe vehicle stopped at the light or not. Figure 1(a), however, shows that it does not work well for quickly switching regimes observed in highway traffic. Another approach is median filtering, which unlike exponential smoothing captures quick changes in regimes as shown on Figure 1(b). However, it will not perform well on an arterial road controlled by traffic signals, since it will be oscillating back and forth between two values. A third approach is to use a piecewise polynomial fit to filter the data. As show on Figure 1(c) this method does perform well, however, the slopes might be underestimated. Thus, out of those three methods the median filter seems to be the most effective.

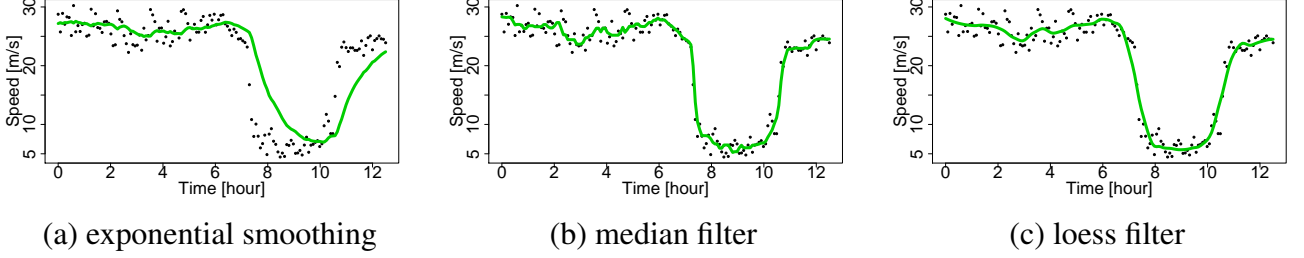


Figure 1: Different filtering algorithms for data pre-processing

An alternative approach to filter the data is to assume that we observe data from the statistical model  $v_i = p(x_i) + e_i$ , where  $p(x)$  is piecewise constant. The fused lasso Tibshirani and Taylor (2011) and  $\ell_1$  trend filtering Kim et al. (2009); Polson and Scott (2014) involves estimating  $p(x) = (p(x_1), \dots, p(x_n))$  at the input points by solving the optimization problem

$$\text{minimize} \quad (1/2)\|y - p(x)\|_2^2 + \lambda\|Dp(x)\|_1.$$

In fused lasso  $D = D^{(1)}$  is the matrix encoding first differences in  $p(x)$ . In  $\ell_1$  trend filtering  $D = D^{(2)}$  is the matrix encoding second differences in  $p(x)$

$$D^{(1)} = \begin{pmatrix} 1 & -1 & 0 & 0 & \cdots & 0 \\ 0 & 1 & -1 & 0 & \cdots & 0 \\ \vdots & & & & \ddots & \vdots \\ 0 & \cdots & & 0 & 1 & -1 \end{pmatrix}, \quad D^{(2)} = \begin{pmatrix} 1 & -2 & 1 & 0 & \cdots & 0 \\ 0 & 1 & -2 & 1 & \cdots & 0 \\ \vdots & & & & \ddots & \vdots \\ 0 & \cdots & & 1 & -2 & 1 \end{pmatrix}.$$

Applying  $D^{(1)}$  to a vector is equivalent to calculating first order differences of the vector. This filter also called 1-dimensional total variation denoising [Rudin et al. (1992)], and hence first order  $\ell_1$  trend filtering estimate  $p(x)$  is piecewise constant across the input points  $x_1, \dots, x_n$ . Higher orders difference operators  $D^{(k)}$ ,  $k > 1$ , correspond to an assumption that the data generating process is modeled by a piece-wise polynomial of order  $k$  function.

Figure 2 shows results of applying  $\ell_1$  to a data measured from a loop-detector on I-55. A computationally efficient algorithms for trend filtering with differentiation operator of any order  $D^{(k)}$  was recently proposed by Ramdas and Tibshirani (2015).

### 3 Chicago Traffic Flow During Special Events

For our empirical study we use data from twenty one loop-detectors installed on a northbound section of Interstate I-55. Those loop-detectors span 13 miles of the highway. A distinct characteristic of traffic flow data is an abrupt change of the mean level. Also we see a lot of variations on the speed measurements. Though, on Figure 1 it might seem that during congested period (6am-9am) the speed variation is small, in reality the signal to noise ratio during congested regime is lower compared to a free flow regime. One approach to treat the noisy data is a probabilistic one. In Polson and Sokolov (2014) authors developed a hierarchical Bayesian model for tracking traffic

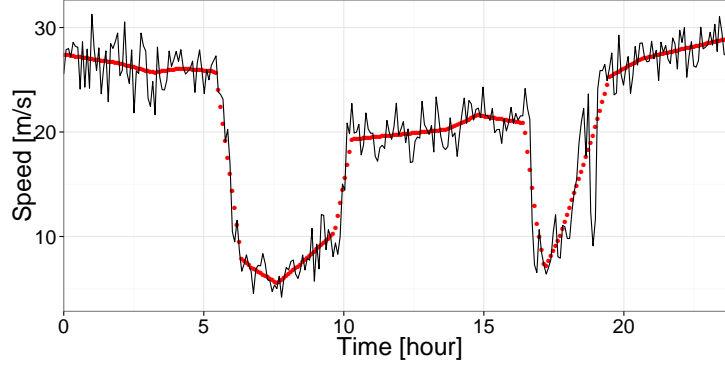


Figure 2:  $\ell_1$  trend filtering based on quadratic loss and penalty that enforces a piecewise line fit.

flows and estimate uncertainty about state variables at any given point in time. However, when information is presented to a user, it has to be presented as a single number, i.e. travel time from my origin to my destination is 20 minutes. A straight forward way to go from a distribution over a traffic state variable (i.e traffic flow speed) to a single number would be to calculate an expected value or a maximum a posteriori.

### 3.1 Traffic Flow on Chicago’s Interstate I-55

One of the key attributes of congestion propagation on a traffic network is the spatial and temporal dependency between bottlenecks. For example, if we consider a stretch of highway and assume a bottleneck, then it is expected that the end of the queue will move from the bottleneck downstream. Sometimes, both the head and tail of the bottleneck move downstream together. Such discontinuities in traffic flow, called shock waves are well studied and can be modeled using a simple flow conservation principles. However, a similar phenomena can be observed not only between downstream and upstream locations on a highway. A similar relationship can be established between locations on city streets and highways Horvitz et al. (2012). Figure 3 shows a time-space diagram of traffic flows on a 13-mile stretch of highway I-55 in Chicago. You can see a clear space-temporal patterns in traffic congestion propagation in both downstream and upstream directions.

Another important aspect of traffic congestion is that it can be “decomposed” into recurrent and non-recurrent factors. For example, a typical commute time from a western suburb to Chicago’s city center on Mondays is 45 minutes. However, occasionally the travel time is 10 minutes shorter or longer. Figure 4 shows summarized data collected from the sensor located eight miles from the Chicago downtown on I-55 north bound, which is part of a route used by many morning commuters to travel from southwest suburbs to the city. Figure 4(a) shows average speed on the selected road segment for each of the five work days, we can see that there is little variation, on average, from one week day to another with travelers most likely to experience delays between 5 and 10am. However, if we look at the empirical probability distribution of travel speeds between 7 and 8 am on the same road segment on Figure 4(b), we see that distribution is bi-modal. We can see that in most of the cases, the speed is around 20 miles per hour, which corresponds to heavy congestion. The free flow speed on this road segment is around 70 miles per hour. Furthermore, the distribution has a heavy left tail. Thus, on many days the traffic is considerably worse, compared to an “average”



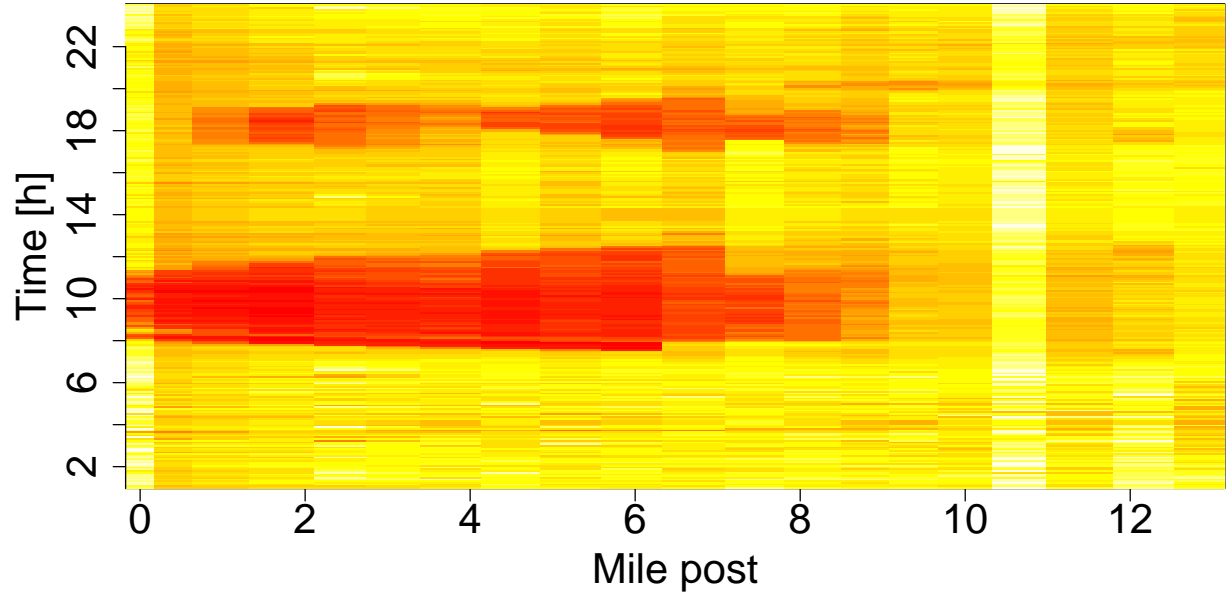


Figure 3: Time-Space diagram that shows traffic flow speed on a 12-mile stretch of I-55. Data measured on from 18 February 2009 (Wednesday). Red means slow speed and light yellow corresponds to free flow speed. The direction of the flow is from 0 to 13.

day.

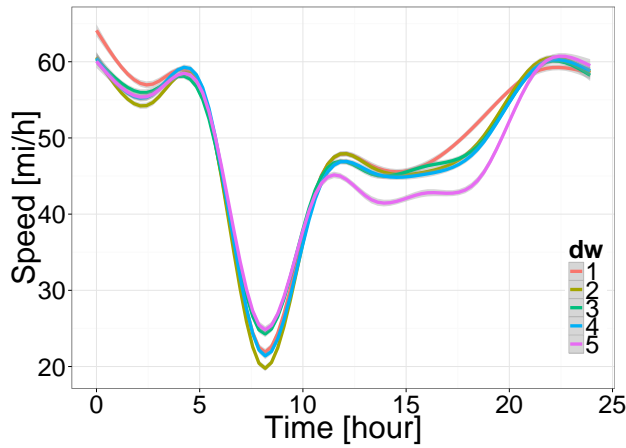
Figure 5(a) shows measurements from all non-holiday Wednesdays in 2009. Solid line and band, represent the average speed and 60% confidence interval correspondingly. Each dot is an individual speed measurement that lies outside of 98% confidence interval. Measurements taken every five minutes, on every Wednesday of 2009, thus we have roughly 52 measurements for each of the five-minute intervals.

We can see that in many cases traffic patterns are very similar from one day to another. However, there are also many days, when there are surprises, both good and bad. A good surprise might happen, for example when schools are closed due to extremely cold weather. A bad surprise might happen due to non-recurrent traffic conditions, such as an accident or inclining weather.

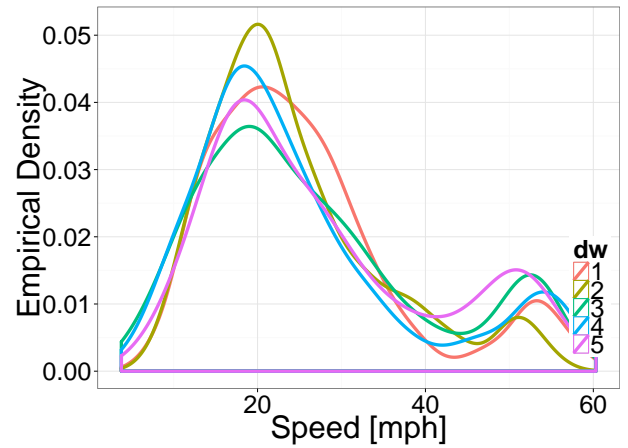
Figure 5(b) illustrates a typical day's traffic flow pattern on Chicago's I-55 highway. This traffic pattern is recurrent, we can see a breakdown in flow speed during the morning peak period, followed by speed recovery. The free flow regimes are usually of little interest to traffic managers.

Figure 6 shows the impact of non-recurrent events. In this case, the traffic speed can significantly deviate from historical averages due to the increased number of vehicles on the road or due to poor road surface conditions. Our goal is to build a statistical model to capturing the sudden regime changes from free flow to congestion and the decline in speed to the recovery regime for both recurrent traffic conditions and non-recurrent ones.

As described above, the traffic congestion usually originates at specific bottlenecks on a network. Therefore, given a bottleneck, our forecast predicts how fast it will propagate on the network. Figure 7, the spatial-temporal relations in traffic data is non linear and we need to model those effects. Thus, the goal is to build deep learning predictors that can capture the nonlinear nature of the traffic flows, as well as spatial-temporal relations with our deep learning model.

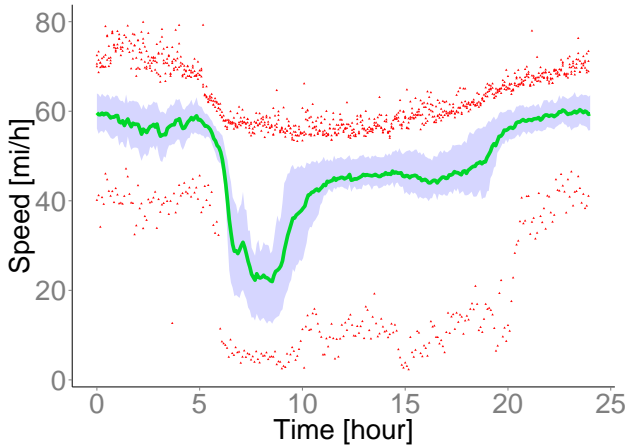


(a) Average speed on work days

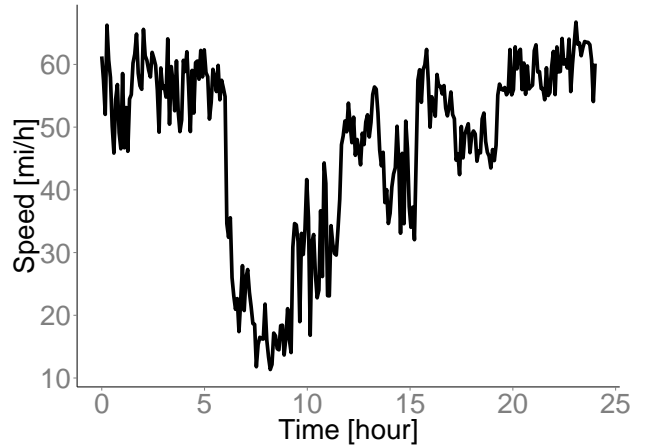


(b) Empirical density for speed, on work days

Figure 4: Analysis of difference in traffic patterns on different days of the week. Left panel (a) shows average speed on work days. Right panel (b) shows Empirical density for speed, for five work days of the week. Calculated based on the data collected between 7 and 8am.

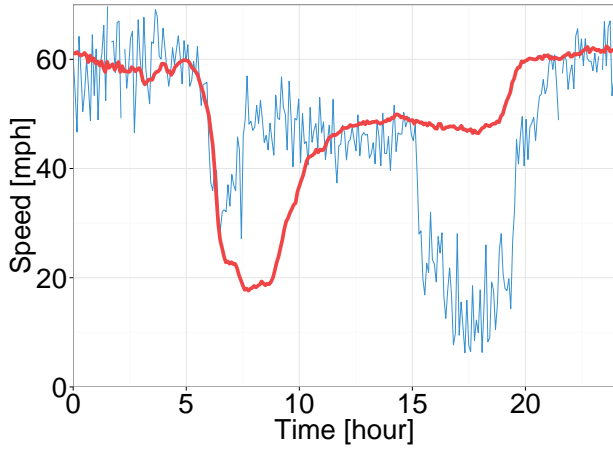


(a) Speed measured on Thursdays

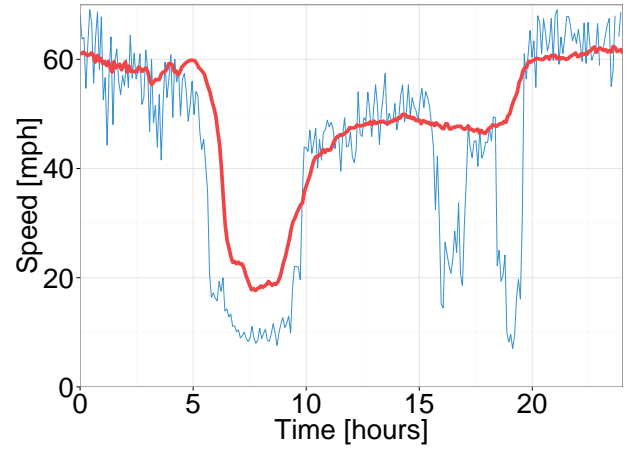


(b) Example of one day speed profile

Figure 5: Recurrent speed profile. Both plots show the speed profile for a segment of interstate highway I-55. Left panel (a) shows the green line, which is the average speed for each of five minute intervals with 60% confidence interval. The red points are measurements that lie outside of 98% confidence interval. Left panel (b) shows an example of one day speed profile from May 14, 2009 (Thursday).

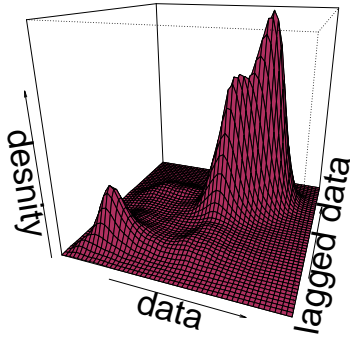


(a) Chicago Bears football game

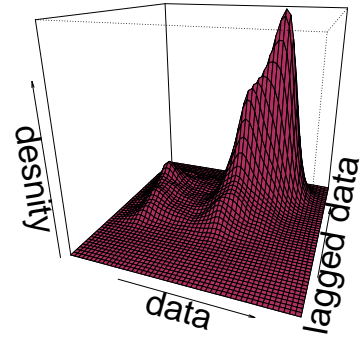


(b) Snow weather

Figure 6: Impact of non-recurrent events on traffic flows. Left panel (a) shows traffic flow on a day when New York Giants played at Chicago Bears on Thursday October 10, 2013. Right panel (b) shoes impact of light snow on traffic flow on I-55 near Chicago on December 11, 2013. On both panels average traffic speed is red line and speed on event day is blue line.



(a) auto-correlation



(b) cross-correlation

Figure 7: Space-time relation between speed measurements. Left panel (a) shows empirical density estimation for the  $(s_n, s_{n-8})$  bivariate random variable, where  $s_n$  is the speed measured at sensor 10 at time  $n$ . Right panel shows empirical density estimation for the  $(s_n^{20}, s_{n-8}^{20})$  bivariate random variable, where  $s_n^{20}$  is the speed measured at sensor 20 at time  $n$ .

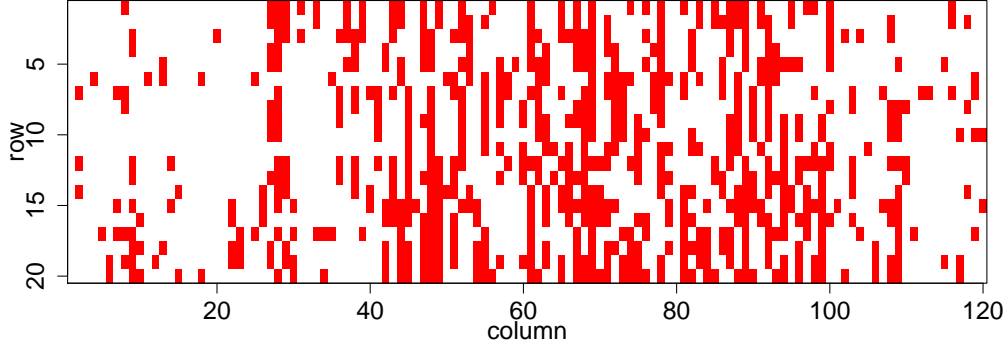


Figure 8: Sparsity patterns of the coefficient matrix found by least angle regression (lars)

### 3.2 Predictor Selection

Our deep learning model will estimate an input-output map  $x_{t+h}^t = \hat{y}_{w,b}(x^t)$ , where  $(w, b)$  index parameters and weights and  $x^t$  is the vector of recent measurement. We will use measurements from ninety consecutive work days. For each of the days we have measurements for every 5 minute interval, resulting in 288 measurements per day per sensor or approximately 55K total measurements.

It is computationally prohibitive to use data from every road segment to develop a forecast for a given location and there is some locality in the casual relations between congestion patterns on different road segments. For example, it is unreasonable to assume that a congested arterial in a central business district can have anything to do with congestion in a remote suburb, sixty miles away. Thus, it might appear logical to select neighbor road segments as predictors. However, it leads to a large number of unnecessary predictors. For example, congestion in one direction (i.e. towards the business district) does not mean there will be congestion in the opposite direction, which leads us to think of the possibility of using topological neighbors as predictors. This approach, also has a major drawback. By using topological neighbors, it is possible not to include important predictors. For example when an arterial road is an alternative to a highway, whose roads will be strongly related, and will not be topological neighbors.

Methods of regularization on another hand allow us an automated way to select predictors. We used least angle regression (lars) procedure to fit  $\ell_1$  regularized loss function (lasso) to find a compact liner model. Figure 8 shows the sparsity pattern of the resulting coefficient matrix.

As we show below, when only covariates selected by lasso were used, the resulting predictor generalizes better and delivers better forecasts.

Another way is to find a sparse neural network model is to apply a dropout operation. Suppose that we have an  $\ell_2$  objective

$$\operatorname{argmin}_{w,b} \|y - \hat{y}_{w,b}(x)\|_2^2.$$

Due to the composite nature of the predictor, we can calculate derivative information  $\nabla_{w,b} l(y, \hat{y}_{w,b}(x))$  using the chain rule via procedure known as backpropagation.

To perform model/variable selection suppose that we dropout any input dimension in  $x$  with probability  $p$ . This replaces the input by  $D \star x$  where  $\star$  denotes element-wise products and  $D$  is a

matrix of  $Ber(p)$  random variables. Marginalize over the randomness, we have a new objective

$$(\hat{w}, \hat{b}) \in \underset{w, b}{\operatorname{argmin}} E_{D \sim Ber(p)} (\|y - \hat{y}_{D \star w, b}(x)\|_2^2),$$

which is equivalent to

$$(\hat{w}, \hat{b}) \in \underset{w, b}{\operatorname{argmin}} \|y - \hat{y}_{w, b}(x)\|_2^2 + p(1 - p)\|\Gamma w\|^2,$$

where  $\Gamma = (\operatorname{diag}(X^\top X))^{\frac{1}{2}}$  and  $X$  is the matrix of observed features. Therefore, the objective function dropout is equivalent to a Bayes ridge regression with a  $g$ -prior, see George (2000).

Then we used model that had a minimal deviance for a validation data set. We used data from 180 days to fit and test the model, we used first half of the selected days for training and the remaining half for testing the models.

### 3.3 Chicago Highway Case Study Results

Having motivated our modeling approaches and described general traffic flow patterns, we evaluate predictive power of sparse linear vector autoregressive (VAR) and deep learning models. We obtained loop detector data from 21 sensors installed on Chicago's Interstate highway I-55 measure in the year of 2013. Those sensors cover a 13-mile stretch of a highway that connects southwest suburbs to Chicago's downtown. We treated missing data by doing interpolation on space, i.e. missing speed measurement  $s_{it}$  for sensor  $i$  at time  $t$  will be amputated using  $(s_{i-1t} + s_{i+1t})/2$ . Days, when the entire sensor network was down were excluded from the analysis. We also excluded public holidays and weekend days.

We compare performance of the deep learning (DL) model with sparse linear vector autoregressive (VAR), combined with several data pre-filtering techniques, namely median filtering with a window size of 8 measurements (M8) and trend filtering with  $\lambda = 15$  (TF15). We also tested performance of the sparse linear model, identified via regularization process. We compared using two metrics, namely  $R$ -squared, which estimates the percent of variance explained by model, and mean squared error (MSE), which measures average of the deviations between measurements and model predictions. To train both models we selected data for 90 days in 2013. We further selected another 90 days for testing data set. We calculated  $R^2$  and MSE for both in-sample (IS) data and out-of-sample (OS) data. Those metrics are shown in Table 1.

	DLL	DLM8L	DLM8	DLTF15L	DLTF15	VARM8L	VARTF15L
IS MSE	13.58	7.7	10.62	12.55	12.59	8.47	15
IS $R^2$	0.72	0.83	0.76	0.75	0.75	0.81	0.7
OS MSE	13.9	8.0	9.5	11.17	12.34	8.78	15.35
OS $R^2$	0.75	0.85	0.82	0.81	0.79	0.83	0.74

Table 1: In sample and out-of-sample metrics for different models. The abbreviations for column headers are as follows: DL = deep learning, VAR = linear model, M8 = media filter preprocessing, TF15 = trend filter preprocessing and L = sparse estimator (lasso). The abbreviations for row headers are as follows: IS = in-sample, MSE = mean squared error and OS = out-of-sample.

Sparse deep learning combined with the median filter pre-processing (DLM8L) shows the best overall performance on the out-of-sample data.

Figure 9 shows performance of both vector auto-regressive and deep learning models for normal day, special event day (Chicago Bears football game) and poor weather day (snow day). We compare our models against the naive constant filter, i.e forecast speed is the same as the current speed. The naive forecast is used by travelers when making route choices before departure. We do it by looking at current traffic conditions and assuming those will hold throughout duration of the planned trip.

Both deep learning (DL) and vector auto-regressive (VAR) models accurately predict morning rush hour congestion on a normal day. However, the vector auto-regressive model mis-predicts congestion during evening rush hour. At the same time deep learning model does predict breakdown accurately but miss-estimates the time of recovery. Both deep learning and liner model outperform naive forecasting, when combined with data pre-processing. However, when unfiltered data is used to fit deep learning combined with sparse linear estimator (DLL) model, their predictive power degrades and get over-performed by a naive forecast. Thus, it shows the importance of using filtered data to develop forecasts.

As was shown in Section 3.1, the data relations are nonlinear. The vector autoregressive model shows surprisingly good performance on the data, and yields an out-of-sample deviance, which is comparable with the one from a deep learning model. However, a deep learning model produces better predictions, for non-recurrent events, as shown for a Bears game and weather day forecasts.

## 4 Discussion

For our time series forecasting, we are using a multilayer feed-forward network, where each layer of nodes receives inputs from the previous layers. The feed-forward network demonstrated an improvement when compared to linear models. There are also other types of networks, that demonstrated superior performance for time series data. For example, the recurrent neural network (RNN) is a class of network where connections between units can form a directed cycle. This creates an internal state that allows to memorize previous data. In our approach, we mimic the behavior of a recurrent neural network by using lagged measurements as predictors. Another class of networks, that are capable of motorizing previous data are the long short term memory (LSTM) network, developed in Hochreiter and Schmidhuber (1997). It is an artificial neural network structure that addresses a problem of the vanishing gradient problem. In a sense, it allows for longer memory and it works even when there are long delays, and it can handle signals that have periodic components of different frequencies. Long short term memory and recurrent neural networks outperformed other methods in numerous applications, such as language learning Gers et al. (2001) and connected handwriting recognition Graves and Schmidhuber (2009).

In this paper we focused on feed forward deep learning models. The hypothesis is that recent observations of traffic conditions (i.e. within last 40 minutes) are stronger predictors rather than historical values, i.e. measurements from 24 hours ago. In other words, future traffic conditions are more similar to current ones as compared to those from previous days. Thus, it allowed us to develop a powerful model by using recent observations as model features. However, we foresee that another class of neural networks, namely the recurrent neural networks can likewise be very applicable to this data set. Those models allow to build more temporally deep networks without

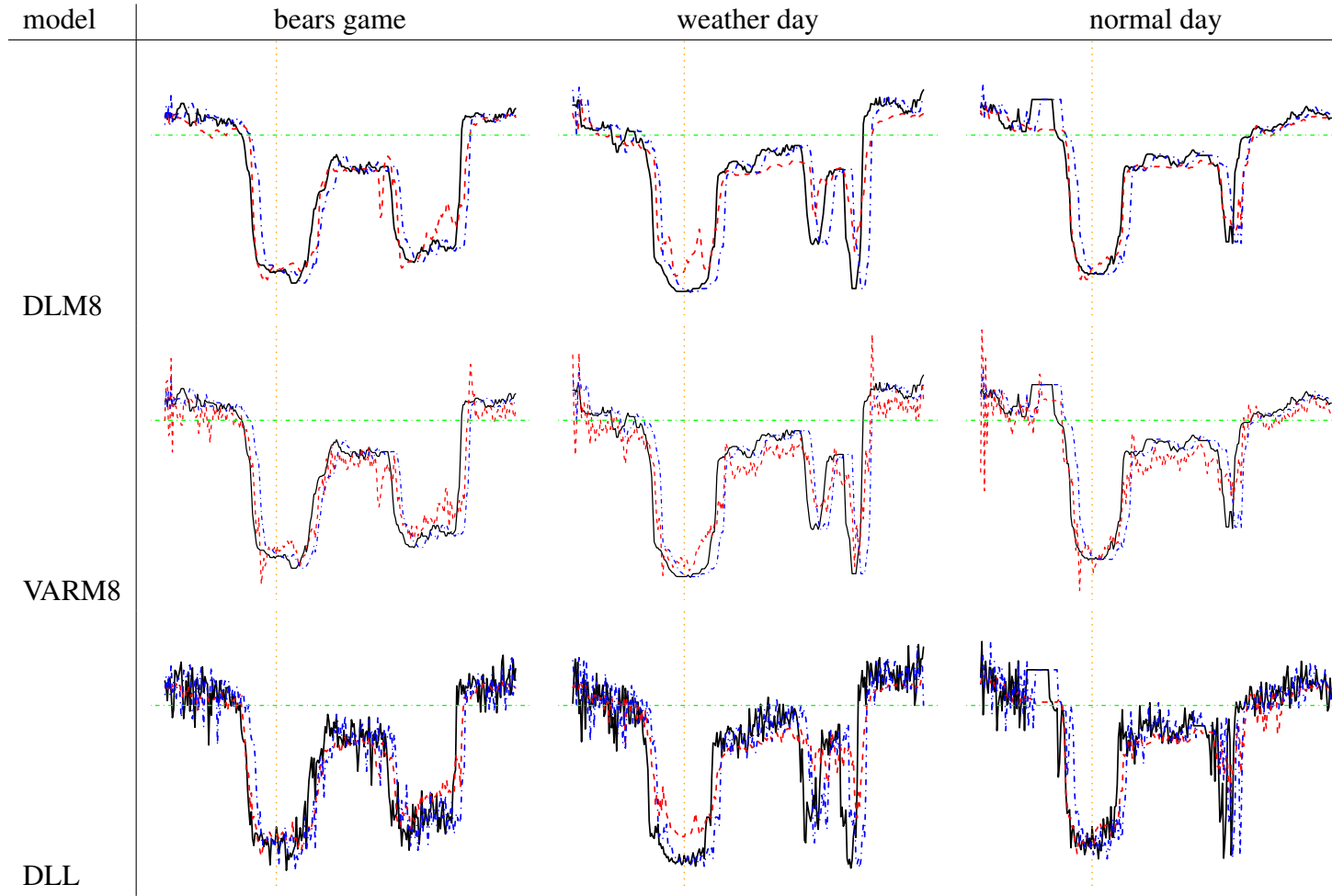


Figure 9: Comparison of the forecasts. On all plots black solid line is the measured data, red dashed line is our model's forty minute forecast and dashed blue line is naive forecast. Green dashed horizontal line is the speed limit (55 mi/h) and vertical orange line is the morning peak hour (8am). First columns compares models for data from Thursday October 10, 2013, the day when Chicago Bears team played New York Giants. The game starts at 7pm and lead to an unusual congestion starting at around 4pm. Second column compares models for data from Wednesday December 11, 2013, the day of light snow. The snow leads to heavier congestion during both, the morning and evening rush hours. Third column compares models for data from Monday October 7, 2013. There were no special events, accidents or inclined weather conditions on this day.

much increase in the number of parameters. They can learn temporal dynamics by mapping an input sequence to a sequence of hidden states and outputs via a recurrent relations

$$\begin{aligned} h_t &= f(w^T[x_t, h_{t-1}] + b_h) \\ \hat{y}_t &= f(w_{hz}^T h_t + b_z). \end{aligned}$$

Compared to the feed-forward deep learning model, given by Equation 1, the hidden layers have an auto-regressive component  $w_{hh}h_{t-1}$ . It leads to a network topology in which each layer represents a time step. We switched to index  $t$  in order to highlight its temporal nature. The equations for a cell of an LSTM model given as follows

$$\begin{aligned} f_t &= \sigma(w_f^T[h_{t-1}, x_t] + b_f) \\ i_t &= \sigma(w_i^T[h_{t-1}, x_t] + b_i) \\ \bar{c}_t &= \tanh(w_c^T[h_{t-1}, x_t] + b_c) \\ c_t &= f_t \star c_{t-1} + i_t \star \bar{c}_t \\ h_t &= o_t \star \tanh(c_t). \end{aligned}$$

The key addition, compared to a recurrent neural network, is the cell state  $c_t$ , the information is added or removed from the memory state via gates defined via a sigmoid function  $\sigma(x) = (1 + e^{-x})^{-1}$  and point-wise multiplication  $\star$ . The first gate  $f_t \star c_{t-1}$ , called the forget gate, allows to throw away some data from the previous cell state. The next gate  $i_t \star \bar{c}_t$ , called the input gate, decides which values will be updated. Then, the new cell state is a sum of the previous cell state, passed through the forgot gate selected components of the  $[h_{t-1}, x_t]$  vector. Thus vector  $c_t$  provides a mechanism for dropping irrelevant information from the past, and adding relevant information from the current time step. The output is the result of the output gate  $o_t \star \tanh(c_t)$ , that returns  $\tanh$  applied to the cell state, with some of the entries removed.

A long short term memory model might potentially improve predictors by utilizing data from the past by memorizing traffic patterns from previous weeks. The long short term memory model allows to automate the identification of the temporal relations in the data, at the cost of larger sets of parameters to be trained.

## References

- Anacleto, O., Queen, C., and Albers, C. J. (2013). Multivariate forecasting of road traffic flows in the presence of heteroscedasticity and measurement errors. *Journal of the Royal Statistical Society: Series C (Applied Statistics)*, 62(2):251–270.
- Bastien, F., Lamblin, P., Pascanu, R., Bergstra, J., Goodfellow, I. J., Bergeron, A., Bouchard, N., and Bengio, Y. (2012). Theano: new features and speed improvements. Deep Learning and Unsupervised Feature Learning NIPS 2012 Workshop.
- Blandin, S., Couque, A., Bayen, A., and Work, D. (2012). On sequential data assimilation for scalar macroscopic traffic flow models. *Physica D: Nonlinear Phenomena*, 241(17):1421–1440.
- Breiman, L. (2003). Statistical modeling: The two cultures. *Quality control and applied statistics*, 48(1):81–82.



- Çetiner, B. G., Sari, M., and Borat, O. (2010). A neural network based traffic flow prediction model. *Mathematical and Computational Applications*, 15(2):269–278.
- Chen, H. and Grant-Muller, S. (2001). Use of sequential learning for short-term traffic flow forecasting. *Transportation Research Part C: Emerging Technologies*, 9(5):319–336.
- Chiou, Y.-C., Lan, L. W., and Tseng, C.-M. (2014). A novel method to predict traffic features based on rolling self-structured traffic patterns. *Journal of Intelligent Transportation Systems*, 18(4):352–366.
- Cook, R. D. (2007). Fisher lecture: Dimension reduction in regression. *Statistical Science*, pages 1–26.
- Dean, J., Corrado, G., Monga, R., Chen, K., Devin, M., Mao, M., Senior, A., Tucker, P., Yang, K., Le, Q. V., et al. (2012). Large scale distributed deep networks. In *Advances in Neural Information Processing Systems*, pages 1223–1231.
- Dellaportas, P., Forster, J. J., Ntzoufras, I., et al. (2012). Joint specification of model space and parameter space prior distributions. *Statistical Science*, 27(2):232–246.
- Diaconis, P. and Shahshahani, M. (1984). On nonlinear functions of linear combinations. *SIAM Journal on Scientific and Statistical Computing*, 5(1):175–191.
- George, E. I. (2000). The variable selection problem. *Journal of the American Statistical Association*, 95(452):1304–1308.
- Gers, F., Schmidhuber, J., et al. (2001). LSTM recurrent networks learn simple context-free and context-sensitive languages. *Neural Networks, IEEE Transactions on*, 12(6):1333–1340.
- Graves, A. and Schmidhuber, J. (2009). Offline handwriting recognition with multidimensional recurrent neural networks. In *Advances in Neural Information Processing Systems*, pages 545–552.
- Hinton, G. E. and Salakhutdinov, R. R. (2006). Reducing the dimensionality of data with neural networks. *Science*, 313(5786):504–507.
- Hochreiter, S. and Schmidhuber, J. (1997). Long short-term memory. *Neural computation*, 9(8):1735–1780.
- Horvitz, E. J., Apacible, J., Sarin, R., and Liao, L. (2012). Prediction, expectation, and surprise: Methods, designs, and study of a deployed traffic forecasting service. *arXiv preprint arXiv:1207.1352*.
- Kamarianakis, Y., Gao, H. O., and Prastacos, P. (2010). Characterizing regimes in daily cycles of urban traffic using smooth-transition regressions. *Transportation Research Part C: Emerging Technologies*, 18(5):821–840.
- Kamarianakis, Y., Shen, W., and Wynter, L. (2012). Real-time road traffic forecasting using regime-switching space-time models and adaptive LASSO. *Applied stochastic models in business and industry*, 28(4):297–315.

- Karlaftis, M. and Vlahogianni, E. (2011). Statistical methods versus neural networks in transportation research: differences, similarities and some insights. *Transportation Research Part C: Emerging Technologies*, 19(3):387–399.
- Kim, S.-J., Koh, K., Boyd, S., and Gorinevsky, D. (2009).  $\ell_1$  trend filtering. *SIAM review*, 51(2):339–360.
- Kolmogorov, A. (1956). On the representation of continuous functions of several variables as superpositions of functions of smaller number of variables. In *Soviet. Math. Dokl*, volume 108, pages 179–182.
- Lu, Y., Duan, Y., Kang, W., Li, Z., and Wang, F.-Y. (2015). Traffic flow prediction with big data: A deep learning approach. *Intelligent Transportation Systems, IEEE Transactions on*, 16(2):865–873.
- Microsoft Research (2016). Predictive analytics for traffic. [online at <http://research.microsoft.com/en-us/projects/clearflow/>; accessed 14-February-2016].
- Nicholson, W., Matteson, D., and Bien, J. (2014). Structured regularization for large vector autoregressions. *Cornell University*.
- Polson, N. and Sokolov, V. (2014). Bayesian particle tracking of traffic flows. *arXiv preprint arXiv:1411.5076*.
- Polson, N. and Sokolov, V. (2015). Bayesian analysis of traffic flow on interstate i-55: The LWR model. *The Annals of Applied Statistics*, 9(4):1864–1888.
- Polson, N. G. and Scott, J. G. (2014). Mixtures, envelopes, and hierarchical duality. *arXiv preprint arXiv:1406.0177*.
- Polson, N. G., Scott, J. G., and Willard, B. T. (2015). Proximal algorithms in statistics and machine learning. *arXiv preprint arXiv:1502.03175*.
- Ramdas, A. and Tibshirani, R. J. (2015). Fast and flexible admm algorithms for trend filtering. *Journal of Computational and Graphical Statistics*, (just-accepted).
- Ripley, B. D. (1996). *Pattern recognition and neural networks*. Cambridge university press.
- Rudin, L. I., Osher, S., and Fatemi, E. (1992). Nonlinear total variation based noise removal algorithms. *Physica D: Nonlinear Phenomena*, 60(1):259–268.
- Sra, S., Nowozin, S., and Wright, S. J. (2012). *Optimization for machine learning*. Mit Press.
- Tebaldi, C. and West, M. (1998). Bayesian inference on network traffic using link count data. *Journal of the American Statistical Association*, 93(442):557–573.
- Tibshirani, R. J. and Taylor, J. (2011). The solution path of the generalized lasso. *Ann. Statist.*, 39(3):1335–1371.

- TransNet (2016). I-15 express lanes corridor. [online at <http://keepsandiegomoving.com/i-15-corridor/i-15-intro.aspx>; accessed 14-February-2016].
- Van Lint, J., Hoogendoorn, S., and van Zuylen, H. J. (2005). Accurate freeway travel time prediction with state-space neural networks under missing data. *Transportation Research Part C: Emerging Technologies*, 13(5):347–369.
- Vlahogianni, E. I., Karlaftis, M. G., and Golias, J. C. (2005). Optimized and meta-optimized neural networks for short-term traffic flow prediction: a genetic approach. *Transportation Research Part C: Emerging Technologies*, 13(3):211–234.
- Westgate, B. S., Woodard, D. B., on, D. S., Henderson, S. G., et al. (2013). Travel time estimation for ambulances using bayesian data augmentation. *The Annals of Applied Statistics*, 7(2):1139–1161.
- Wold, H. (1956). Causal inference from observational data: A review of end and means. *Journal of the Royal Statistical Society. Series A (General)*, pages 28–61.
- Work, D. B., Blandin, S., Tossavainen, O.-P., Piccoli, B., and Bayen, A. M. (2010). A traffic model for velocity data assimilation. *Applied Mathematics Research eXpress*, 2010(1):1–35.
- Zheng, W., Lee, D.-H., and Shi, Q. (2006). Short-term freeway traffic flow prediction: Bayesian combined neural network approach. *Journal of transportation engineering*, 132(2):114–121.